

SSZ-45: A High-Silica Zeolite with Small Pore Openings, Large Cavities, and Unusual Adsorption Properties

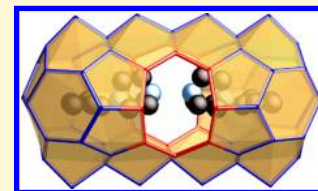
Stef Smeets,[†] Dan Xie,^{*,‡} Lynne B. McCusker,^{*,†} Christian Baerlocher,[†] Stacey I. Zones,[‡] Joshua A. Thompson,[‡] Howard S. Lacheen,[‡] and Hua-Min Huang[‡]

[†]Laboratory of Crystallography, ETH Zurich, CH-8093 Zurich, Switzerland

[‡]Chevron Energy Technology Company, Richmond, California 94802, United States

S Supporting Information

ABSTRACT: Separations of small molecules such as CO₂ and N₂ or CH₄ and CO₂ are key to many industrial processes, but it is not always easy to find a molecular sieve that can discriminate between these molecules and withstand the harsh conditions often required. The high-silica zeolite SSZ-45, which was synthesized using *N*-cyclopentyl-diazabicyclooctane as the structure directing agent (SDA), was found to exhibit excellent thermal stability and rather unusual adsorption properties under pressure. That is, it has potential in the area of small molecule separations. Of particular interest, therefore, was the structural basis for its peculiar adsorption behavior. The relatively complex silicate framework structure of SSZ-45 was determined from a combination of synchrotron powder diffraction and rotation electron diffraction data. Once the framework was known, it was possible to locate the organic SDA in the cavities and to better understand its contribution to the formation of the zeolite. Here we describe the synthesis of SSZ-45, the analysis of its structure, and the subsequent investigation of its small molecule separation properties.



INTRODUCTION

High-silica small-pore zeolites are of particular interest for gas separation applications, because they offer not only a fine molecular sieving property but also high thermal stability, even in the presence of water. Many routes to the synthesis of such materials have been explored over the years, and these have been nicely summarized by Moliner et al.¹ The hydrophobic nature of high-silica zeolites is especially important when separations have to be carried out in the presence of water.² Zeolites with lower Si/Al ratios will absorb the polar water molecules preferentially over other components such as CO₂ in the gas stream, and this limits their suitability for many industrial processes. Very few small-pore zeolites have this hydrophobicity, and those that do are usually synthesized using the so-called fluoride route (i.e., in the presence of HF), which is not ideal for industrial-scale production. Here we describe the synthesis, structure analysis, and adsorption properties of SSZ-45, a high-silica zeolite with small pores and large cavities that was produced without using fluoride.

SSZ-45 was discovered some years ago in a zeolite synthesis screening program that was focused on using diazabicyclooctane (DABCO) derivatives as structure directing agents (SDA).³ We had found in earlier experiments that the diquatery SDA formed by linking two DABCO units with a methylene chain could be used to crystallize the zeolites SSZ-16 (framework type code AFX⁴),^{5,6} SSZ-41⁷ or VPI-8 (VET),⁸ depending on the synthesis parameters used. With the benzyl derivative of the tertiary nitrogen on DABCO, we discovered the borosilicate SSZ-42 (IFR).⁹ A similar synthesis (ITQ-4) was reported about the same time by the Corma group.¹⁰ Continuing this approach, the C5 derivatives, based upon either an iso- or cyclopentyl group (Figure 1) were investigated. Using

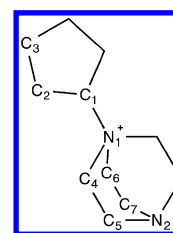


Figure 1. Schematic drawing of the *N*-cyclopentyl-DABCO structure directing agent used in the synthesis of SSZ-45.

very-high-silica synthesis conditions, the novel phase SSZ-45, with well-formed crystallites (Figure 2), was produced.³ The integrity of the crystalline solid remained after thermal calcination to remove the C5-DABCO guest molecules, so its adsorption properties were investigated for possible application.

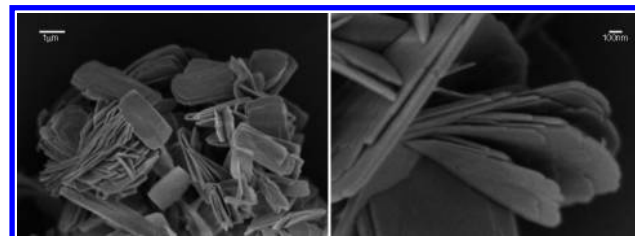


Figure 2. Scanning electron micrographs of SSZ-45 showing the platelet morphology of the crystallites.

Received: April 3, 2014
 Revised: May 15, 2014
 Published: May 30, 2014

■ EXPERIMENTAL SECTION

Synthesis of SSZ-45. 4.6 mL (3 mmol) of the cyclopentyl-DABCO solution (0.65 M), 0.75 g of 1 N KOH, and 6 mL of water were added to the Teflon cup of a 23 mL Parr 4745 reactor to yield a clear, basic solution. The silica was then supplied by adding 0.92 g of TOSOH HUA 390. This source is a highly dealuminated FAU-type material and is typically a reactive source of silica containing just a small amount of Al (Si/Al ratio of ca. 250). It provides a route for making zeolites with some Al in essentially all-silica synthesis conditions. This Al can be useful in learning about catalytic tendencies. The mixture (molar composition, 15.25 SiO₂:0.03 Al₂O₃:3 SDAOH:0.71 KOH:630 H₂O) was sealed and heated at 160 °C in an oven equipped with a rotating spit operating at 43 rpm for 2 weeks. The product was then recovered, and found by X-ray powder diffraction (XPD) to be SSZ-45. CHN analysis (Galbraith Laboratories, Inc., Knoxville, TN, USA) of the product yielded 7.88 wt % C, 1.53 wt % H, and 1.65 wt % N (C_{10.6}H_{2.5}N₂), indicating that the SDA (C₁₁H₂₁N₂) was intact with approximately 0.04 SDA/Si.

Gas Adsorption Experiments. Adsorption experiments with CO₂, CH₄, and N₂ at 30 °C were performed on a volumetric gas adsorption system, SETARAM PCTPro-2000 instrument. This instrument is equipped with a low- and high-pressure transducer for measurement between 0.001 and 60 bar total pressure. SSZ-45 samples were activated by heating to 250 °C under vacuum for 8 h. The same procedure was repeated following each adsorption measurement. Free space measurements were performed using He as an inert gas to obtain the volume of the system.

X-ray Powder Diffraction Data Collection. Synchrotron XPD data were collected on the Materials Science beamline at the Swiss Light Source (wavelength, 0.99822 Å; MYTHEN II detector) in Villigen, Switzerland.¹¹

Rotation Electron Diffraction Data Collection. Three-dimensional electron diffraction data were collected on eight crystals of SSZ-45 (each ca. 100 nm in size) using the rotation electron diffraction (RED) technique.¹² The RED software was installed on a JEOL 2010 microscope operating at 200 kV, and data were collected over a tilt range of ±50° with a tilt step 0.2° and an exposure time of 2 s. Relatively large tilt steps had to be used for these measurements, because the software to perform the finer tilts by tilting the electron beam had not yet been implemented. As a result, the RED data were not of optimal quality.

■ RESULTS AND DISCUSSION

Structure Analysis. The autoindexing routine in *Topas*¹³ was used to index the XPD data. Although an orthorhombic unit cell ($a = 13.7129$ Å, $b = 35.1924$ Å, $c = 22.1253$ Å) was found, some small peaks were not indexed and the space group proved to be ambiguous (*Fmmm* or *Bmmm* or a subgroup thereof). Therefore, intensities were extracted using the Pawley profile-fitting procedure¹⁴ in *Topas*¹⁵ assuming several different space groups. Each of these data sets was then used as input to the powder charge-flipping algorithm¹⁶ in *Superflip*.¹⁷ However, no clear structure emerged. In retrospect, one can see that some features of the maps resemble those of the structure, but they were not sufficiently well defined to allow interpretation.

Therefore, the RED technique for collecting three-dimensional single-crystal ED data on tiny crystallites was brought into play in the hope that such data would provide some additional information. All eight RED data sets could be indexed on an *F*-centered orthorhombic unit cell similar to the one found for the XPD pattern. No violations of the *F*-centering condition were observed. Reflection intensities were then extracted for each data set using the RED software,¹⁸ and the best two of these were merged (53% coverage) for further analysis.

Attempts to solve the structure directly from these data using *Superflip* failed. However, when some nonoverlapping reflections from laboratory XPD data were added to the RED data, a layered structure could be discerned. By adding a layer of isolated four-rings (four tetrahedral SiO₄ units, each sharing two O atoms to form a ring) between the layers, a fully connected framework structure could be constructed. The simulated XPD pattern for this model was found to match the measured one quite well.

In an independent attempt to solve the structure, the zeolite-specific structure solution program *Focus*¹⁹ was applied to the SSZ-45 synchrotron XPD data. Reflection intensities were extracted assuming the *Fmmm* symmetry indicated by the RED data, and the best solution proved to be the same as the one derived above.

The *Focus* algorithm was originally written to work with XPD data, but in view of the advances in ED technology, it was modified in 2013 to accept ED data.²⁰ As one of the tests of the modified version of the program, the less-than-ideal RED data for SSZ-45 were also tried. Again, the solution found most frequently was identical to the one found with XPD data. The main difference is that the solutions with RED data were produced in just 80 min of CPU time, while those with XPD data required 20 h. A summary of the two *Focus* runs is given in Table 1. It appears that poor, incomplete single-crystal ED data

Table 1. Details of the Solutions of the Structure of SSZ-45 Using Focus with XPD and RED Data^a

	XPD	RED
reflections measured	982	4326
unique reflections	982	782
overlapping reflections	795	0
reflections used	200	200
d_{\min} (Å) of reflections used	1.18	1.05
completeness ^b (%)	100	53
trials	155 147	8000
correct solutions	108	142
total CPU time (min)	1200	80
Sec/correct solution	667	34

^aThe computations were performed in parallel on a 2010 Mac Pro equipped with dual 2.4 GHz Quad-Core Intel Xeon processors.

^bCompleteness of the full data set up to d_{\min} corresponding to the reflections used.

are better than high-quality XPD data (with a high degree of overlap) for structure solution with *Focus*. However, XPD data are still essential for structure completion and refinement. For charge flipping, on the other hand, the incompleteness of the ED data seems to have a more detrimental effect.

The fact that the same framework structure (Figure 3), with 10 Si atoms in the asymmetric unit, was found with three different methods gave us confidence that it was likely to be correct. Bridging O atoms were added to the model, and then the geometry was optimized using the distance-least-squares program DLS-76.²¹ The framework structure was later identified as being the same as that reported 3 years ago for ERS-18.²² That structure was solved by Zanardi and co-workers using *Focus* and high-resolution synchrotron XPD data. The framework has now been assigned the code EEI by the Structure Commission of the International Zeolite Association.⁴

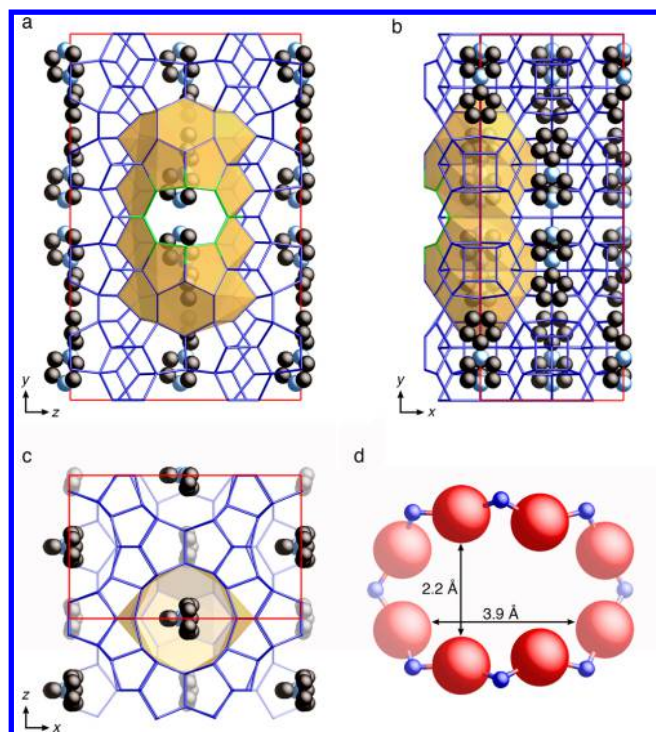


Figure 3. Projections of the structure of SSZ-45 along the (a) *a* axis, (b) *c* axis, and (c) *b* axis showing the framework structure (O atoms omitted for clarity) and the arrangement of the organic SDA cations. One large cavity with its small pore opening has been highlighted in each projection. The top of the cavity in c has been removed to show the diameter of the cavity. (d) Eight-ring pore with the delimiting O atoms and its effective dimensions (O atom radius of 1.35 Å subtracted).

Structure refinement of SSZ-45 with the Rietveld method²³ was initiated using the DLS-optimized atomic coordinates and the program *Topas*.¹⁵ Geometric restraints were applied to all unique bond distances and angles. To locate the SDA within the pore structure, a model of the organic cation was generated and optimized using the energy minimization routine in *Jmol*,²⁴ and then added to the SSZ-45 model as a rigid body. Its approximate position and orientation in the channel system were then found via the simulated-annealing algorithm in *Topas*. In this way, two symmetry-equivalent cations were positioned in each of the long cavities in the framework structure. Their locations and orientations were then refined, allowing internal rotation around the C1–N1 bond (see Figure 1).

In the space group *Fmmm*, two of the 19 O atoms lie on a center of symmetry, producing Si–O–Si angles of 180°. By reducing the symmetry to *Fmm2*, the positions of these two O atoms could be refined freely, leading to more favorable Si–O–Si angles and an improved profile fit. The symmetry reduction also resolved some, but not all, of the disorder of the SDA cations. During the course of the refinement, the SDA seemed to align itself along the mirror plane perpendicular to the short axis, so the rigid body description was changed to a geometrically restrained molecule with C1, N1, C6, and C7 fixed on the mirror plane. This resolved the remaining disorder of the SDA. In the final stages of the refinement, H atoms were added in their geometrically expected positions. The OH[−] counterions could not be located. A March-type correction for

the anisotropic line broadening²⁵ was applied along the [031] direction.

The final structure, with 59 non-hydrogen atoms in the asymmetric unit (18 Si, 32 O, 7 C, and 2 N) converged with the agreement values $R_I = 0.008$ and $R_{wp} = 0.145$ ($R_{exp} = 0.038$) (Table 2). The main differences in the profile fit (Figure 4) can

Table 2. Crystallographic Data for the Structure Solution and Rietveld Refinement of SSZ-45

composition	$[(C_{11}H_{21}N_2)_8(OH)_8][Si_{200}O_{400}]$	R_I	0.008
space group	<i>Fmm2</i>	R_{wp}	0.145
<i>a</i> (Å)	13.7195(1)	R_{exp}	0.038
<i>b</i> (Å)	35.2245(6)	observations	13 479
<i>c</i> (Å)	22.1362(1)	reflections	1273
2θ range (deg)	3.0–55.0	parameters	214
wavelength (Å)	0.99822(1)	restraints	277

be attributed to problems with the description of the peak shape. The refined composition agrees well with the chemical analysis.

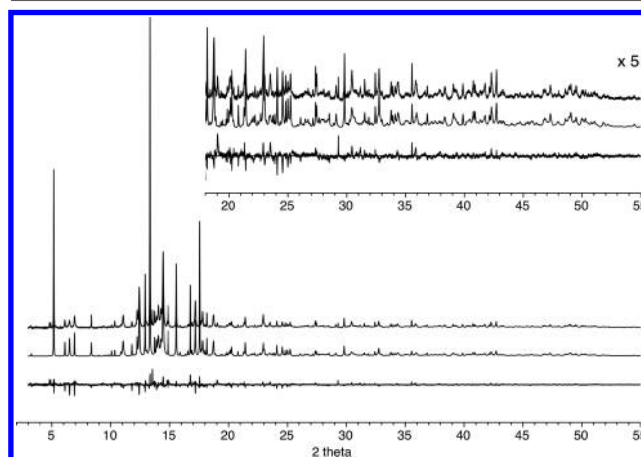


Figure 4. Observed (top), calculated (middle), and difference (bottom) profiles for the Rietveld refinement of SSZ-45. The intensity scale of the inset has been increased by a factor of 5 to show more detail.

The framework structure of SSZ-45 is closely related to those of nonasil (NON²⁶), EU-1 (EUO²⁷), and NU-87 (NES²⁸). This relationship has been described very nicely by Zanardi and co-workers in their description of ERS-18,²² so only the SSZ-45 framework structure with its small oval pore opening and large cavity is depicted in Figure 3. The pore system consists of one-dimensional eight-ring channels running parallel to the short *a* axis with large side pockets extending along the long *b* axis on both sides of the channel. The framework geometry of SSZ-45 appears to be more regular than that reported for ERS-18. This may be a result of the different synthesis conditions that produced a purer phase in the case of SSZ-45, the effect of using a lower symmetry for the structure refinement, or because the SSZ-45 sample was in its as-synthesized form. The calcination of ERS-18 prior to structure analysis may have caused a reduction in the sample integrity.

The SDAs fit well into the large cavity of SSZ-45 (Figure 3b). Unlike the 6-azoniaspiro[5,5]undecane (C₁₀H₂₀N) SDA used in the synthesis of ERS-18, the SSZ-45 SDA has a mirror plane that matches the symmetry of the framework. It is also larger

($C_{11}H_{21}N_2$) and less symmetric than the ERS-18 SDA. These differences may have allowed the framework structure to form with less strain. This is the second case we are aware of in which two bulky organic cations have paired up within a zeolite cavity. The other instance is SSZ-52, which also has an elongated cavity with eight-ring-openings.²⁹

The effective pore opening of the oval eight-ring is only ca. $2.2 \text{ \AA} \times 3.9 \text{ \AA}$ (Figure 3d), but the cavity itself is approximately 5.6 \AA in diameter and 19.8 \AA in length. In other words, SSZ-45 has a small pore opening that can discriminate between small molecules but a large cavity that gives the zeolite a high adsorption capacity.

Gas Adsorption and Separation. Initial microporosity experiments using N_2 and Ar showed only a small micropore uptake ($0.056 \text{ cm}^3/\text{g}$), but when CO_2 was used as the probe molecule, a significantly higher porosity was obtained. The t -plot volume was nearly double that estimated from the N_2 and Ar experiments. Micropore volume calculated using the Dubinin–Radushkevich method yielded even higher values ($0.14 \text{ cm}^3/\text{g}$). CO_2 has a smaller kinetic diameter (3.3 \AA) than N_2 (3.6 \AA) or Ar (3.4 \AA), and as the experiments were carried out at higher temperature, it also had increased kinetic energy to enter the eight-ring pores of SSZ-45. The lower but nonzero micropore filling observed for N_2 and Ar may indicate the presence of structural defects or pore blocking. CO_2 adsorption has been used previously to determine zeolite porosity. For example, García-Martínez et al. demonstrated that CO_2 adsorbed reversibly in the Na form of zeolite A (LTA) at 273 K and that the estimated micropore volume was larger than that obtained with N_2 , because CO_2 could better access the small pores.³⁰ Similar results were obtained by Ridha et al. on a K-exchanged chabazite (CHA) material.³¹

Gas adsorption measurements were performed at $30 \text{ }^\circ\text{C}$ to explore the potential of SSZ-45 for application in small-molecule (CO_2 , CH_4 , and N_2) separations (Figure 5). Because of the high Si:Al ratio, there is no steep uptake of CO_2 at low partial pressures. This behavior has also been observed for other high-silica zeolite materials.^{32,33} However, when the pressure is increased to 30 bar or more, where the CO_2 uptake is nearly saturated in other small-pore zeolites (e.g., SSZ-13),³⁴

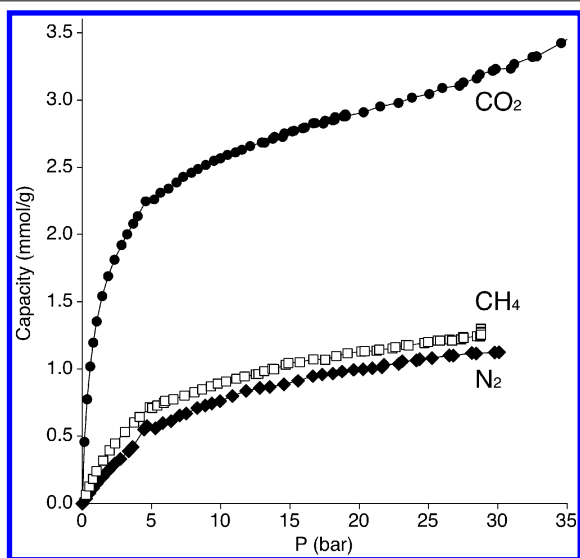


Figure 5. Adsorption isotherms of CO_2 , N_2 , and CH_4 in SSZ-45 at $30 \text{ }^\circ\text{C}$.

that in SSZ-45 continues to increase and the uptake curve becomes even steeper. Interestingly, the larger CH_4 molecule was also adsorbed, indicating some flexibility in the oval eight-ring pore opening.³⁵ While the flexibility may change the expected diffusion rates of small molecules into the zeolite, it is unlikely to affect the equilibrium adsorption behavior^{36,37} for these small gas molecules. The behavior of the adsorption isotherms of CH_4 and N_2 for SSZ-45 is more closely related to that of ETS-4, another material with oval eight-rings,³⁸ than to that of DDR- and LTA-type zeolites, because they have similar total adsorption capacities and Henry's constants for both N_2 and CH_4 .

Ideal adsorbed solution theory (IAST),³⁹ a thermodynamic method for predicting the equilibrium adsorption behavior of a material for gas mixtures, has been applied successfully to CO_2 adsorption in zeolites.⁴⁰ It was used to assess the expected multicomponent adsorption behavior of SSZ-45 for three different gas compositions relevant for flue gas separations (CO_2/N_2) and for biogas and natural gas separations (CO_2/CH_4). The results of these calculations (Table 3) indicate that

Table 3. IAST Calculations for SSZ-45 with Different Gas Mixtures Containing CO_2 , N_2 , and CH_4 at $30 \text{ }^\circ\text{C}$

gas 1:gas 2	P (bar)	mole fraction		selectivity
		gas 1	gas 2	
$CO_2:N_2$	1.0	0.15	0.85	24.3
$CO_2:CH_4$	10.0	0.50	0.50	24.1
$CO_2:CH_4$	40.0	0.10	0.90	24.2

the small aperture and large cavity of SSZ-45 may result in adsorption or membrane separation properties for CO_2/CH_4 that are superior to those of other high-silica zeolites (e.g., DDR- and MFI-type), which have been investigated extensively for this purpose.^{32,33,41} SSZ-45 has 3.5 times their adsorption selectivity for CO_2/CH_4 and similar selectivity for CO_2/N_2 .^{41,42} SSZ-45 is also likely to have high diffusion selectivity, which would make it a promising candidate for membrane separations, but further investigation is needed to clarify the nature of the flexibility of the eight-ring.¹ Furthermore, because of its hydrophobicity, SSZ-45 (with Si:Al > 150) could be attractive for adsorptive or membrane separations in which water is present in the gas phase. Here it would have a significant advantage over the commonly used aluminosilicate zeolites, such as Na-13X.⁴³

CONCLUSION

The high-silica zeolite SSZ-45, synthesized using a DABCO derivative as the SDA, exhibits excellent thermal stability and unusual adsorption properties that might be put to use in small-molecule separation processes. Elucidation of its complex framework structure, with 18 Si atoms in the asymmetric unit, was approached in three different ways, using both X-ray powder diffraction and rotation electron diffraction data. Of particular note is the evident power of combining even poor RED data with the zeolite-specific structure solution program *Focus*. The framework structure proved to have the same topology as ERS-18,²² but in the case of SSZ-45 the geometry of the framework is less strained and it was possible to locate the SDA within the pores and refine its position. Access to the large $19.6 \text{ \AA} \times 5.6 \text{ \AA}$ cavity is limited by small oval eight-rings, and this makes the zeolite an attractive one for small-molecule separations. Preliminary adsorption experiments are promising,

and further investigations of the suitability of SSZ-45 for gas separation application are in progress.

■ ASSOCIATED CONTENT

● Supporting Information

Crystallographic information file (cif) of the refined structure of SSZ-45. This material is available free of charge via the Internet at <http://pubs.acs.org>. File also available from the Fachinformationszentrum Karlsruhe, 76344 Eggenstein-Leopoldshafen, Germany (fax, +49 7247 808 666; e-mail, crysdta@fiz-karlsruhe.de) on quoting the depository number CSD-427318.

■ AUTHOR INFORMATION

Corresponding Authors

*(D.X.) E-mail: dan.xie@chevron.com. Phone: +1 510 242 6452.

*(L.B.M.) E-mail: mccusker@mat.ethz.ch. Phone: +41 44 632 3721.

Funding

This work was supported by the Swiss National Science Foundation and the Chevron Energy Technology Co.

Notes

The authors declare no competing financial interest.

■ ACKNOWLEDGMENTS

We thank the beamline scientists on the Materials Science Beamline at the SLS in Villigen, Switzerland for their assistance with the powder diffraction measurement and Tom Rea at Chevron ETC for the RED data collection.

■ REFERENCES

- (1) Moliner, M.; Martínez, C.; Corma, A. *Chem. Mater.* **2014**, *26*, 246.
- (2) Pham, T. D.; Xiong, R.; Sandler, S. I.; Lobo, R. F. *Microporous Mesoporous Mater.* **2014**, *185*, 157.
- (3) Yuen, L. T.; Zones, S. I. U.S. Patent 6,033,643, 2000.
- (4) Three-letter framework type codes (boldface capital letters) for all zeolites mentioned in the text are given in parentheses. They can be found in: Baerlocher, C.; McCusker, L. B.; Olson, D. H. *Atlas of Zeolite Framework Types*, 6th revised ed.; Elsevier: Amsterdam, 2007; or at <http://www.iza-structure.org/databases/>.
- (5) Zones, S. I. U.S. Patent 4,508,837, 1985.
- (6) Lobo, R. F.; Zones, S. I.; Medrud, R. C. *Chem. Mater.* **1996**, *8*, 2409.
- (7) Zones, S. I.; Santilli, D. S. U.S. Patent 5,656,149, 1997.
- (8) Yoshikawa, M.; Zones, S. I.; Davis, M. E. *Microporous Mater.* **1997**, *11*, 127.
- (9) Chen, C. Y.; Finger, L. W.; Medrud, R. C.; Kibby, C. L.; Crozier, P. A.; Chan, I. Y.; Harris, T. V.; Beck, L. W.; Zones, S. I. *Chem.—Eur. J.* **1998**, *4*, 1312.
- (10) Cambor, M. A.; Corma, A.; Villaescusa, L. A. *Chem. Commun. (Cambridge, U. K.)* **1997**, 749.
- (11) Willmott, P. R.; Meister, D.; Leake, S. J.; Lange, M.; Bergamaschi, A.; Boge, M.; Calvi, M.; Cancellieri, C.; Casati, N.; Cervellino, A.; Chen, Q.; David, C.; Flechsig, U.; Gozzo, F.; Henrich, B.; Jaggi-Spielmann, S.; Jakob, B.; Kalichava, I.; Karvinen, P.; Krempasky, J.; Ludeke, A.; Luscher, R.; Maag, S.; Quitmann, C.; Reinle-Schmitt, M. L.; Schmidt, T.; Schmitt, B.; Streun, A.; Vartiainen, I.; Vitins, M.; Wang, X.; Wulschleger, R. *J. Synchrotron Radiat.* **2013**, *20*, 667.
- (12) Zhang, D.; Oleynikov, P.; Hovmöller, S.; Zou, X. D. *Z. Kristallogr.* **2010**, *225*, 94.
- (13) Coelho, A. A. *J. Appl. Crystallogr.* **2003**, *36*, 86.
- (14) Pawley, G. S. *J. Appl. Crystallogr.* **1981**, *14*, 357.

(15) Coelho, A. A. *TOPAS-Academic*, v4.1; Coelho Software: Brisbane, Australia, 2007.

(16) Baerlocher, C.; McCusker, L. B.; Palatinus, L. Z. *Kristallogr.* **2007**, *222*, 47.

(17) Palatinus, L.; Chapuis, G. *J. Appl. Crystallogr.* **2007**, *40*, 786.

(18) Wan, W.; Sun, J. L.; Su, J.; Hovmöller, S.; Zou, X. D. *J. Appl. Crystallogr.* **2013**, *46*, 1863.

(19) Grosse-Kunstleve, R. W.; McCusker, L. B.; Baerlocher, C. *J. Appl. Crystallogr.* **1997**, *30*, 985.

(20) Smeets, S.; McCusker, L. B.; Baerlocher, C.; Mugnaioli, E.; Kolb, U. *J. Appl. Crystallogr.* **2013**, *46*, 1017.

(21) Baerlocher, C.; Hepp, A.; Meier, W. M. *DLS-76, a program for the simulation of crystal structures by geometric refinement*; Institute of Crystallography and Petrography, ETH Zurich: Zurich, Switzerland, 1977.

(22) Zanardi, S.; Millini, R.; Frigerio, F.; Belloni, A.; Cruciani, G.; Bellussi, G.; Carati, A.; Rizzo, C.; Montanari, E. *Microporous Mesoporous Mater.* **2011**, *143*, 6.

(23) Rietveld, H. M. *J. Appl. Crystallogr.* **1969**, *2*, 65.

(24) Hanson, R. M. *J. Appl. Crystallogr.* **2010**, *43*, 1250.

(25) March, A. Z. *Kristallogr.* **1932**, *81*, 285.

(26) Marler, B.; Dehnbestel, N.; Eulert, H.-H.; Gies, H.; Liebau, F. *J. Inclusion Phenom.* **1986**, *4*, 339.

(27) Briscoe, N. A.; Johnson, D. W.; Shannon, M. D.; Kokotailo, G. T.; McCusker, L. B. *Zeolites* **1988**, *8*, 74.

(28) Shannon, M. D.; Casci, J. L.; Cox, P. A.; Andrews, S. J. *Nature* **1991**, *353*, 417.

(29) Xie, D.; McCusker, L. B.; Baerlocher, C.; Zones, S. I.; Wan, W.; Zou, X. D. *J. Am. Chem. Soc.* **2013**, *135*, 10519.

(30) García-Martínez, J.; Cazorla-Amorós, D.; Linares-Solano, A. *Stud. Surf. Sci. Catal.* **2000**, *128*, 485.

(31) Ridha, F. N.; Yang, Y.; Webley, P. A. *Microporous Mesoporous Mater.* **2009**, *117*, 497.

(32) Zhu, W.; Hrabanek, P.; Gora, L.; Kapteijn, F.; Moulijn, J. A. *Ind. Eng. Chem. Res.* **2006**, *45*, 767.

(33) Palomino, M.; Corma, A.; Rey, F.; Valencia, S. *Langmuir* **2010**, *26*, 1910.

(34) Hudson, M. R.; Queen, W. L.; Mason, J. A.; Fickel, D. W.; Lobo, R. F.; Brown, C. M. *J. Am. Chem. Soc.* **2012**, *134*, 1970.

(35) Awati, R. V.; Ravikovitch, P. I.; Sholl, D. S. *J. Phys. Chem. C* **2013**, *117*, 13462.

(36) Vlught, T. J. H.; M. Schenk, M. *J. Phys. Chem. B* **2002**, *106*, 12757.

(37) García-Sánchez, A.; Dubbeldam, D.; Calero, S. *J. Phys. Chem. C* **2010**, *114*, 15068.

(38) Majumdar, B.; Bhadra, S. J.; Marathe, R. P.; Farooq, S. *Ind. Eng. Chem. Res.* **2011**, *50*, 3021.

(39) Myers, A. L.; Prausnitz, J. M. *AIChE J.* **1965**, *11*, 121.

(40) Ohlin, L.; Grahn, M. *J. Phys. Chem. C* **2014**, *118*, 6207.

(41) Himeno, S.; Tomita, T.; Suzuki, K.; Yoshida, S. *Microporous Mesoporous Mater.* **2007**, *98*, 62.

(42) van den Bergh, J.; Zhu, W.; Gascon, J.; Moulijn, J. A.; Kapteijn, F. *J. Membr. Sci.* **2008**, *316*, 35.

(43) Wang, Y.; LeVan, M. D. *J. Chem. Eng. Data* **2010**, *55*, 3189.